

Theoretical Modeling of Plasmon Dispersions in 2D Heterostructures

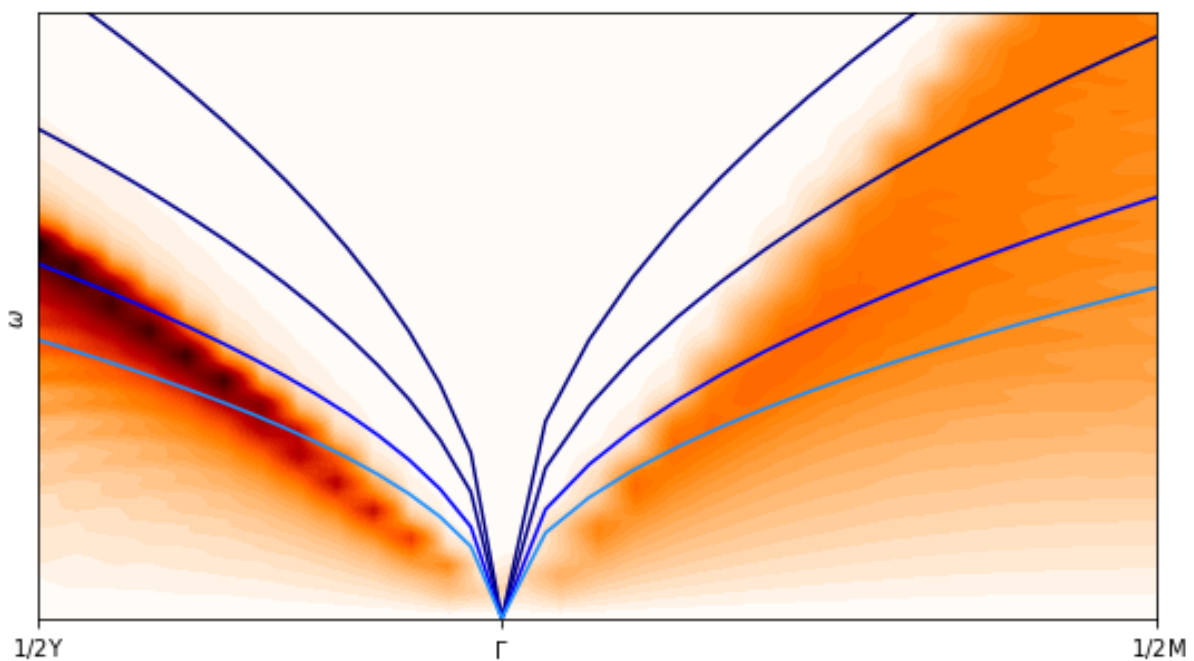
Bachelor Thesis

Author: Anne Riewald

Supervisor: Dr. Malte Rösner

Second reader: Prof. Dr. Alex Khajetoorians

July 29th 2020



Theory of Condensed Matter
Institute of Molecules and Materials
Radboud University

Contents

1	Introduction	2
2	Theory	3
2.1	Screening	3
2.2	Plasmon dispersions	3
2.3	Dielectric function	4
2.3.1	Metallic polarization	4
2.3.2	WFCE Coulomb interaction	5
2.4	Electron Energy Loss Spectrum (EELS)	7
3	Implementation	8
4	Results	10
4.1	Simple 2D plasmons	10
4.2	Interband screening	12
4.3	Varying height	13
4.4	External screening	14
4.5	Anisotropy	15
5	Conclusion and outlook	17
A	Code	18

1 Introduction

Plasmons are collective electronic charge density excitations in a system [1], and belong to the group of fundamental collective many-body excitations of a solid state system, such as phonons (lattice vibrations) or magnons (spin waves). They depend on properties like the ground state of a system and are therefore influenced by changes to the energy of system. Plasmons have been found to affect superconductivity [2], and show potential for use in optics, solar cells and sensors [3]. Also, plasmonic nanostructures have been shown to enhance the optical properties of graphene [4]. Thus, plasmons are important for the understanding and tuning of material properties.

In this study, we will use the Electron Energy Loss Spectrum $EELS_q(\omega)$ to allow us to study how plasmonic excitations are affected by material parameters such as 2D layer height, metallic, interband, and anisotropic screening. We start from a 2D electron gas model and build this up to a realistic 2D metallic layer setup. Here, the WFCE approach [5] is used to handle the screening channels in the Coulomb interaction instead of in the polarization. Finally, we will present the first proof for the possibility to induce anisotropic plasmonic excitations in an isotropic 2D layer using anisotropic substrate screening.

2 Theory

2.1 Screening

The Coulomb interaction between two electrons is the most fundamental interaction in a solid state system. From classical electrostatics we know the bare Coulomb interaction $V_{\mathbf{q}}$ [6] in 2D¹ to be defined by:

$$V_{\mathbf{q}} = \frac{e^2}{2\varepsilon_0 A} \cdot \frac{1}{|\mathbf{q}|}, \quad (1)$$

where e is the electron charge, ε_0 is the vacuum permittivity, and A is the surface of a unit cell. However, in a solid state system, there are vast amounts (on the order of 10^{23} and up) of electrons present. All of them should be accounted for in the Coulomb interaction term, so the bare Coulomb interaction will be affected. Taking in every individual electron would lead to a highly non-trivial many body system. So instead, to solve this we will stay focused on two electrons, and see how the additional electrons change the bare Coulomb interaction between them. The additional electrons will rearrange themselves under the potential of the electron pair, and this will lead to a polarization of the environment in which our two electrons live. This polarization will screen the bare Coulomb interaction. The new, fully screened Coulomb interaction $W_{\mathbf{q}}$ [6] can now be defined as :

$$W_{\mathbf{q}} = \frac{V_{\mathbf{q}}}{\varepsilon_{\mathbf{q}}(\omega)}, \quad (2)$$

where $V_{\mathbf{q}}$ is the bare Coulomb interaction and $\varepsilon_{\mathbf{q}}(\omega)$ is the dielectric function, which will be further examined in section 2.3.

2.2 Plasmon dispersions

Plasmons are collective electronic charge density excitations in a system between Coulomb coupled electrons. These excitations are especially pronounced in metals, where they can be seen as the collective oscillation of the "electronic sea". The plasmon dispersion [7] is defined by the dielectric function $\varepsilon_{\mathbf{q}}(\omega)$ of the the system;

$$\varepsilon_{\mathbf{q}}(\omega_{\mathbf{q}}) \equiv 0, \quad (3)$$

where $\omega_{\mathbf{q}}$ is the plasmon dispersion. Plasmons therefore play a crucial role in the understanding, and the definition of the frequency dependent properties of the screened Coulomb interaction $W_{\mathbf{q}}(\omega)$.

At the plasmonic excitations, where the dielectric function is zero, the screened Coulomb interaction diverges. This is the way we could visualise the plasmonic excitations. However, we can not measure the screened Coulomb interaction directly. So to visualise the plasmon excitations we will shift our focus from the fully screened Coulomb interaction to the dielectric function (section 2.3) and the EELS (section 2.4).

¹For an even more realistic picture, the 2D bare Coulomb interaction could be defined as [6]: $V_{\mathbf{q}} = \frac{e^2}{2\varepsilon_0 A} \cdot \frac{1}{q(1+\gamma q)}$. Here γ describes the affect of the effective height of the material layer on short wavelengths, which becomes important only at large wave vectors. Because we are mainly interested in small wave vectors, we omit this factor.

2.3 Dielectric function

The dielectric function $\varepsilon_{\mathbf{q}}(\omega)$ [7] of a material is dependent on the frequency ω and momentum wave vector \mathbf{q} and is defined as:

$$\varepsilon_{\mathbf{q}}(\omega) = 1 - V_{\mathbf{q}} \cdot \Pi_{\mathbf{q}}(\omega), \quad (4)$$

where $V_{\mathbf{q}}$ is the bare Coulomb interactions in the material, and $\Pi_{\mathbf{q}}(\omega)$ is the polarization.

The first situation of interest, is the one where only metallic screening is considered. This screening is caused by the electrons in the metallic bands of the electronic band structure. The polarization is then only defined by metallic band interactions ($\Pi_{\mathbf{q}}^{metal}$). For the Coulomb interaction, the bare Coulomb interaction, as explained in section 2.1, can be used. However, screening in a real material can not be completely described by metallic band polarization.

A more realistic representation can be achieved by also including non-metallic bands. This changes the screening and that will be reflected in the polarization: for $\Pi_{\mathbf{q}}(\omega)$, the sum of $\Pi_{\mathbf{q}}^{metal}(\omega)$ and $\Pi_{\mathbf{q}}^{internal}(\omega)$ should be taken. $\Pi_{\mathbf{q}}^{internal}(\omega)$ is the polarization caused by screening from non-metallic internal bands. The dielectric function now changes to:

$$\varepsilon_{\mathbf{q}}(\omega) = 1 - V_{\mathbf{q}} \cdot (\Pi_{\mathbf{q}}^{metal}(\omega) + \Pi_{\mathbf{q}}^{internal}(\omega)). \quad (5)$$

If we now imagine not only an isolated layer in vacuum, but also a substrate surrounding it, external screening has to be taken into account. Another polarization term now enters into the equation:

$$\varepsilon_{\mathbf{q}}(\omega) = 1 - V_{\mathbf{q}} \cdot (\Pi_{\mathbf{q}}^{metal}(\omega) + \Pi_{\mathbf{q}}^{internal}(\omega) + \Pi_{\mathbf{q}}^{external}(\omega)). \quad (6)$$

These polarization terms are quite tedious to evaluate, making the dielectric function hard to calculate. However, one can adjust the bare Coulomb interaction to account for the change in screening instead of changing the polarization term. The metallic polarization is then the only polarization needed, and we can replace the dielectric function equations above by:

$$\varepsilon_{\mathbf{q}}(\omega) = 1 - U_{\mathbf{q}} \cdot \Pi_{\mathbf{q}}^{metal}(\omega), \quad (7)$$

where $U_{\mathbf{q}}$ is the partially screened Coulomb interaction and $\Pi_{\mathbf{q}}^{metal}(\omega)$ is the metal polarization. The partially screened Coulomb interaction $U_{\mathbf{q}}$ is proportional to the bare Coulomb interaction $V_{\mathbf{q}}$ divided by an effective dielectric function $\epsilon_{\mathbf{q}}$, which renders the screening, and will be further explained in section 2.3.2.

2.3.1 Metallic polarization

The polarization is the relative tendency of a system to redistribute its charge when subjected to an external electromagnetic perturbation. The metallic polarization [7] can be expressed in the Random Phase Approximation by:

$$\Pi_{\mathbf{q}}(\omega) = \sum_{\mathbf{k}} \frac{f(\mathbf{k} + \mathbf{q}) - f(\mathbf{k})}{\omega + i\delta + E(\mathbf{k} + \mathbf{q}) - E(\mathbf{k})} \quad (8)$$

This is called the Lindhard function. As mentioned before, this function is used to evaluate the metal polarization, so it uses only a single screening channel, namely the metallic screening. In the function, $f(\mathbf{k})$ is a Fermi function for energy $E(\mathbf{k})$ and δ is a small broadening parameter.

2.3.2 WFCE Coulomb interaction

As explained before, instead of calculating all the different polarization terms, the screening interactions will be incorporated into the partially screened Coulomb interaction term $U_{\mathbf{q}}$ which is defined by:

$$U_{\mathbf{q}} = \frac{V_{\mathbf{q}}}{\epsilon_{\mathbf{q}}}, \quad (9)$$

where $V_{\mathbf{q}}$ is the bare Coulomb interaction and $\epsilon_{\mathbf{q}}$ is an effective dielectric function. This effective dielectric function handles the screening channels not taken into account by the metallic polarization. As mentioned before, screening can also be inserted into the material via external channels, so $\epsilon_{\mathbf{q}}$ must also be dependent on the surrounding material. In Figure 1, we sketch the situation we will examine in this study ².

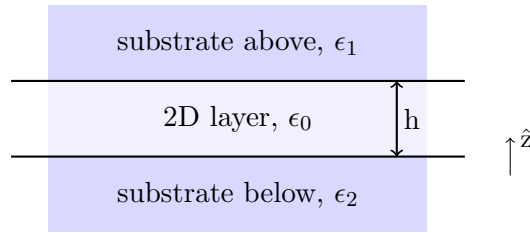


Figure 1: Representation of the 2D material layer with the substrate above and below. The dielectric constant of the layers are ϵ_0 , ϵ_1 and ϵ_2 . The height of the layer is h .

A 2D material layer with a substrate above and below it is used. We take the 2D plane to be very large compared to a single unit cell such that boundary conditions are negligible. The effective dielectric function [5] is now given by:

$$\epsilon_{\mathbf{q}} = \frac{\epsilon_0[1 - \tilde{\epsilon}_1\tilde{\epsilon}_2e^{-2|q|h}]}{1 + [\tilde{\epsilon}_1 + \tilde{\epsilon}_2]e^{-|q|h} + \tilde{\epsilon}_1\tilde{\epsilon}_2e^{-2|q|h}}, \quad (10)$$

where ϵ_0 , ϵ_1 and ϵ_2 are the dielectric constant of the 2D layer, substrate above and substrate below respectively. The dielectric constants are a measure of the polarizability of each material layer. h is the height of the 2D layer, and $\tilde{\epsilon}_i$ is given by:

$$\tilde{\epsilon}_i = \frac{\epsilon_0 - \epsilon_i}{\epsilon_0 + \epsilon_i}. \quad (11)$$

In Figure 2 $\epsilon_{\mathbf{q}}$ is plotted for different dielectric constants and heights.

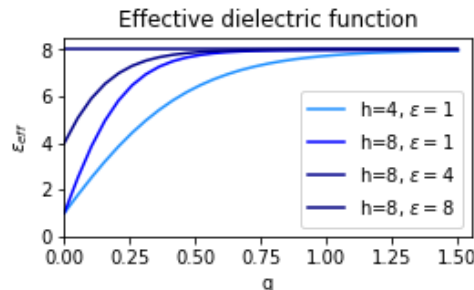


Figure 2: Plots of the effective dielectric function $\epsilon_{\mathbf{q}}$, for $\epsilon_0 = 8$, $\epsilon_1 = \epsilon_2 = \epsilon$ and 2D layer height h .

²The substrate above and below look the same in the picture, but in practice (and in the formulas) they do not have to be the exact same material. Actually, in practice it is more often the case that they are different. However, for the scope of this study we will take them, in calculations, as the same.

Here, we see that for larger momenta all plots reach $\epsilon_{\mathbf{q}} = \epsilon_0$. Also note that the value of the effective dielectric function at $\mathbf{q} = 0$ equals $(\epsilon_1 + \epsilon_2)/2$. Lastly, we notice that the effective dielectric function calculated with a larger 2D layer height reaches $\epsilon_{\mathbf{q}} = \epsilon_0$ already for a smaller momentum. A larger effective dielectric function results in a smaller partially screened Coulomb interaction. And using equations (3) and (7), this results in a decrease in plasmonic energy.

We also want to be able to handle anisotropy. The dielectric constant of a layer then has a directional dependence. It no longer has one component for all directions, but a distinct x- and y-component, $\epsilon_i = (\epsilon_{i,x}, \epsilon_{i,y})$. It now needs to be transformed before it can be put in equation (10). This is done using the following equation, for each momentum vector \mathbf{q} :

$$\epsilon_i = \frac{\left| \begin{pmatrix} \epsilon_{i,x} & 0 \\ 0 & \epsilon_{i,y} \end{pmatrix} \cdot \begin{pmatrix} q_x \\ q_y \end{pmatrix} \right|}{|\mathbf{q}|} \quad (12)$$

This equation scales the dielectric constant in X direction with the X coordinate in momentum space, and similarly for the Y direction. This means that if we calculate the dielectric constant ϵ_i , we take into account if the \mathbf{q} point is more or less polarizable in a certain direction depending on where it is in space. Also, note that if $\epsilon_{i,x} = \epsilon_{i,y} = \epsilon$, ϵ_i will result ϵ , which returns the dielectric constant to the isotropic situation.

2.4 Electron Energy Loss Spectrum (EELS)

In practice, the EELS is measured by shooting a beam of electrons, which are similar in kinetic energy, at a material. These electrons will scatter, and the amount of energy loss can be measured via an electron spectrometer. These energy losses can then be interpreted to find out the cause of the specific energy loss, e.g. phonon or plasmon excitations. [8]

The EELS [7] can also be calculated, as:

$$EELS_{\mathbf{q}}(\omega) = -Im \left[\frac{1}{\varepsilon_{\mathbf{q}}(\omega)} \right] \quad (13)$$

Here, $\varepsilon_{\mathbf{q}}(\omega)$ is the dielectric function from equation (7). Also, the full EELS can be defined as the sum over the EELS for all \mathbf{q} points divided by the number of \mathbf{q} points:

$$EELS_{full}(\omega) = -\frac{1}{\#\mathbf{q}} \sum_{\mathbf{q}} Im \left[\frac{1}{\varepsilon_{\mathbf{q}}(\omega)} \right] = \frac{1}{\#\mathbf{q}} \sum_{\mathbf{q}} EELS_{\mathbf{q}}(\omega) \quad (14)$$

The dielectric function consists of a real and a imaginary part. If we write $\varepsilon_{\mathbf{q}}(\omega)$ as $\varepsilon_{Re} + i\varepsilon_{Im}$, we can use that to rewrite equation (13):

$$EELS = -Im \left[\frac{1}{\varepsilon_{Re} + i\varepsilon_{Im}} \right] = -Im \left[\frac{\varepsilon_{Re}}{\varepsilon_{Re}^2 + \varepsilon_{Im}^2} - \frac{i\varepsilon_{Im}}{\varepsilon_{Re}^2 + \varepsilon_{Im}^2} \right] = \frac{\varepsilon_{Im}}{\varepsilon_{Re}^2 + \varepsilon_{Im}^2} \quad (15)$$

From this, we see that the EELS will maximize for very small ε_{Re} and ε_{Im} . This corresponds to a plasmon dispersion (remember equation (3)), so the EELS can be used to visualise plasmonic excitations.

Note that while $\varepsilon_{Re} = 0$ is necessary to define the plasmon dispersion [9] (it is a real world problem), ε_{Im} should be as small as possible to maximize the EELS. With decreasing ε_{Im} , the EELS increases in intensity and we get a stronger plasmon excitation. When ε_{Im} is increased, the intensity of the EELS decreases and we dampen the plasmon excitation.

ε_{Im} is only controlled by the imaginary part of the polarization. All other quantities constructing the dielectric function are real. This means that the polarization is the only term controlling the dampening of the plasmonic excitations. The more the plasmon energy differs from the imaginary part of the polarization, the less dampening there is and the stronger the plasmon excitation becomes.

3 Implementation

The theory of section 2 will be implemented using a tight binding model defined on a square lattice with a lattice spacing $a = 4 \text{ \AA}$. A single s orbital is located at position $(0,0)$ in the unit cell. For the electrons, only nearest neighbour hopping is allowed. In Figure 3, a representation is given of the square lattice examined in the model, and of its corresponding first Brillouin zone in momentum space. Here, the high symmetry points of the lattice are also declared.



Figure 3: (a) Section of the real space square lattice with lattice spacing $a = 4 \text{ \AA}$. (b) First Brillouin zone of the square lattice in momentum space with spacing $b = 2\pi/a$. The symbols represent important high symmetry points in the Brillouin zone.

The region of interest in this lattice is around the zero momentum point Γ . This is where the momentum vectors are small. To efficiently visualise this region the paths $1/2X - \Gamma - 1/2Y$ and $1/2Y - \Gamma - 1/2M$ will be used.

The tight binding Hamiltonian of the square lattice [10] is defined by:

$$\mathcal{H}_R = -t \sum_{\sigma <i,j>} (c_{\sigma i}^\dagger c_{\sigma j} + c_{\sigma j}^\dagger c_{\sigma i}), \quad (16)$$

where t is the hopping parameter, which is set to 1.0 in the program. $c_{\sigma i}^\dagger$ creates a fermion with spin $\sigma \in \{1, -1\}$ on lattice site i , and $<i,j>$ denotes summation over nearest neighbours i and j [11]. An alternative form of this Hamiltonian [10] can be defined for momentum space:

$$\mathcal{H}_q = \sum_{\mathbf{q}, \sigma} \epsilon(\mathbf{q}) c_{\sigma \mathbf{q}}^\dagger c_{\sigma \mathbf{q}}, \quad (17)$$

where $\epsilon(\mathbf{q})$ is the momentum space dispersion. For a square lattice the electronic dispersion [12] is given by:

$$\epsilon(\mathbf{q}) = -2t \cos(\mathbf{q}a) = -2t [\cos(q_x a) + \cos(q_y a)] \quad (18)$$

The electronic dispersion $\epsilon(\mathbf{q})$, and the density of states (DOS) for the tight binding model, are shown in Figure 4. The density of states describes the number of states occupied at each energy level.

The DOS in Figure 4a is symmetric and peaks at an energy of 0 eV. The peak corresponds to $\epsilon = \mu$ (the Fermi level), and originates from the Van Hove singularity at the Y point (see electronic dispersion in Figure 4b). The DOS is less smooth than expected. As the blue and orange line in Figure 4a, the model created has a 60×60 \mathbf{q} grid. Comparing the orange and green lines in Figure 4a, we see that increasing the number of points in space, smoothens the curves, i.e. would improve the correctness of our model.

The model is implemented using Python and makes use of the module TPRF (two-particle

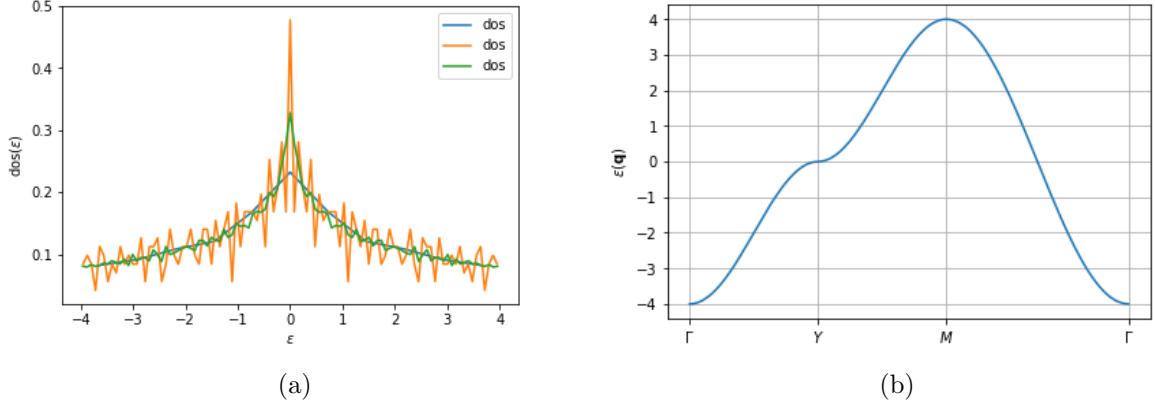


Figure 4: (a) *Density of states*, and (b) *Electronic dispersion*. Both plots are created using a tight binding Hamiltonian with hopping parameter $t = 1$ and chemical potential $\mu = 0$ eV (bands are half full). In the DOS plot, the lines differ from each other in the number of points taken to make the plot. The blue and orange line took 11 and 101 points over energy respectively, and both 60×60 q points. The green line took also 101 points over the energy, but 200×200 q points.

response function tools)[11] from TRIQS (Toolbox for Research on Interacting Quantum Systems). TPRF is for example used to implement the polarization. Here, the function `triqs_tprf.lattice.lindhard_chi00_fk()` is used. This function takes as arguments $\epsilon(\mathbf{q})$, mesh, β , μ , and δ . The mesh and dispersion $\epsilon(\mathbf{q})$ are also created using TPRF functions. The broadening parameter δ is the same as in equation (8), and is set to 0.1. The chemical potential, and inverse temperature are set to $\mu = 2.0$ eV and $\beta = 5.0$ eV $^{-1}$. Remember that $\beta = 1/k_B T$, so $T \approx 2325$ K. For the complete implemented code, see the git repository [13]. A couple of self implemented functions can be found in Appendix A with some comments.

4 Results

4.1 Simple 2D plasmons

In this section, the simplest screening case will be considered. Only the metallic band screening will be taken into account. This is realized by looking at cases where the dielectric constants of the material and both substrate layers are equal ($\epsilon_0 = \epsilon_1 = \epsilon_2 = \epsilon$). Increasing the dielectric constants simultaneously corresponds to increasing the metallic screening.

To get a feeling of the overall change in EELS when the metallic screening is increased, the full EELS is plotted in Figure 5. The full EELS is the sum over all momentum vectors \mathbf{q} of the EELS per frequency divided by the number of momentum vectors.

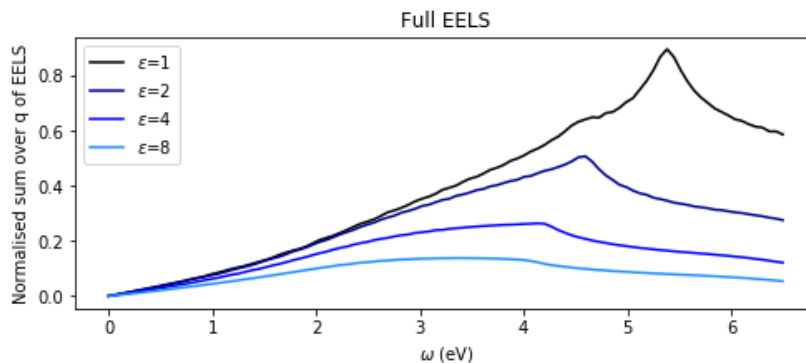


Figure 5: *The full EELS for varying metallic screening (induced by different values for the dielectric constant ϵ).*

In Figure 5, the full EELS decreases for larger screening. A decrease of the intensity of the EELS can be interpreted as a dampening of the plasmon. Also, the peak of the full EELS shifts to a lower frequency for larger screening. This can be interpreted as a decrease of the plasmon frequency.

Now, we can look at the region for small momenta \mathbf{q} . The situation of only metallic screening is in theory similar to a free electron gas where we mostly look at low momentum electron scattering. Because of this, the dispersion relation can be approximated by $\omega_{\mathbf{q}} = c\sqrt{|\mathbf{q}|}$ for small momenta, which is the plasmon dispersion of a perfect 2D electron gas [14]. In Figure 6, EELS plots are shown for different metallic dielectric constants $\epsilon_0 = \epsilon_1 = \epsilon_2 = \epsilon$. For each plot, a dispersion relation is fitted by hand, where we ensure a perfect fit especially for the small momenta.

Note that the height of the material layer is not important in this case. Looking at equations (10) and (11), when all dielectric constants (ϵ_0 , ϵ_1 and ϵ_2) are equal, the effective dielectric function reduces to $\epsilon_q = \epsilon_0$, which is no longer dependent on the height (or the wave vector). For completeness however, the height is given in the figure.

From the figure, it is clear that, for increased screening, the fitted dispersion relations do not completely follow the corresponding EELS for larger wave vectors. To try to explain this, the fitted dispersion relations found in Figure 6 are plotted over the imaginary part of the polarization. This is shown in Figure 7.

For larger wave vectors, the dispersion plots intersect the polarization continuum, especially for the smaller dispersions. This happens at similar wave vector and energy as where the dispersion relation fit no longer corresponds to the EELS in Figure 6. This means that the plasmon

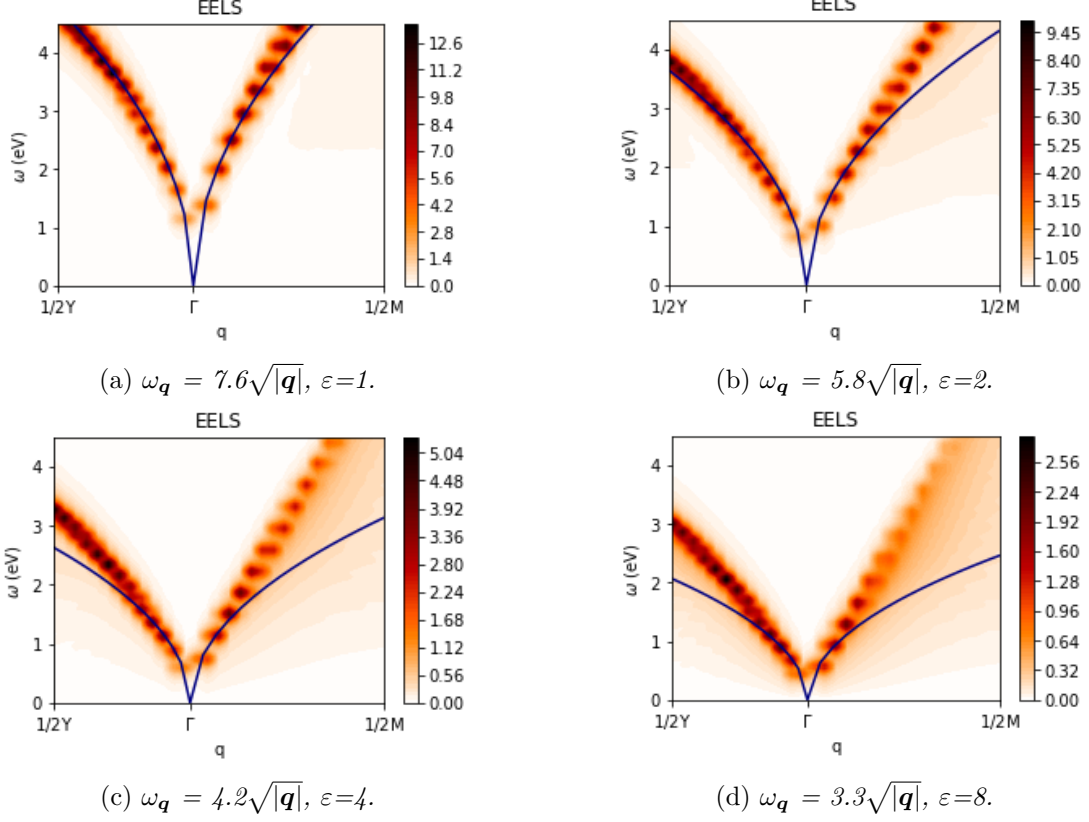


Figure 6: Each figure shows the $EELS_q(\omega)$ as a colormap along paths towards high symmetry points in the square lattice. The corresponding fitted dispersion relation ω_q is plotted in blue. The dielectric constant ε ($=\varepsilon_0 = \varepsilon_1 = \varepsilon_2$) and ω_q are given in the description. The height of the layer is 8 \AA .

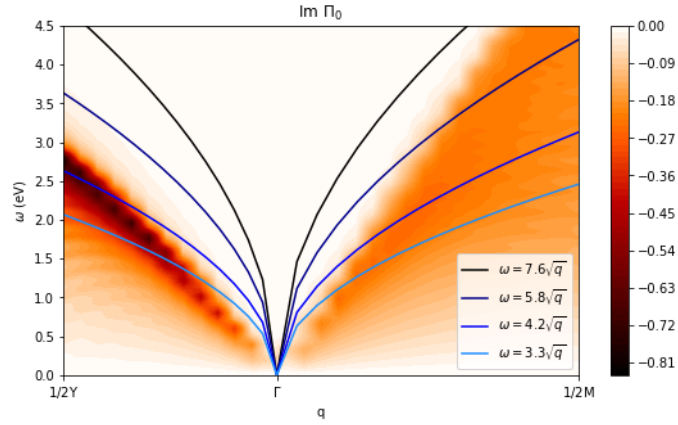


Figure 7: Imaginary part of the polarization overlain with different estimated dispersion relations.

is likely strongly damped and thus not well defined anymore.

4.2 Interband screening

In this section, the effect of the internal screening channel on the plasmon dispersion will be examined. This is achieved by keeping the height h and the dielectric constants of the substrate layers ($\epsilon_1 = \epsilon_2 = 1$) constant while varying the dielectric constant of the 2D layer ϵ_0 . The results are shown in Figure 8.

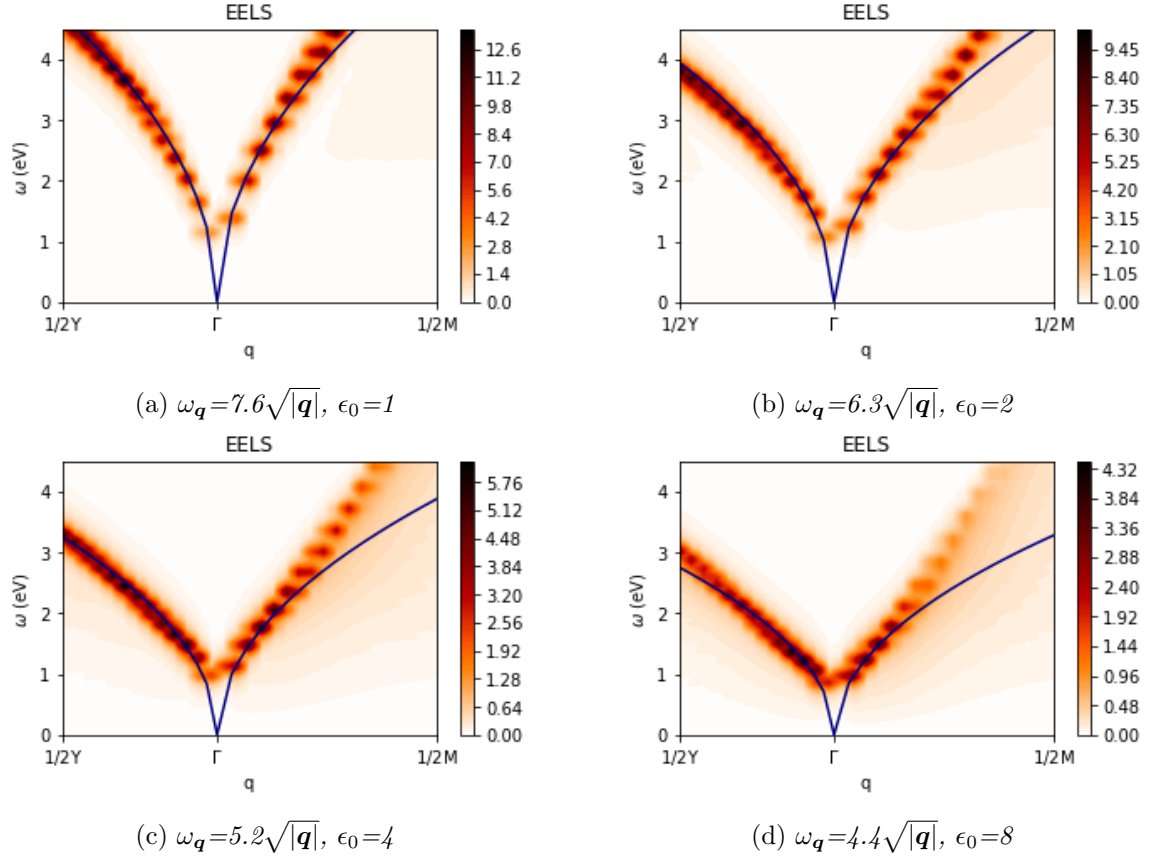


Figure 8: Each figure shows the $EELS_{\mathbf{q}}(\omega)$ as a colormap along paths towards high symmetry points in the square lattice. The corresponding fitted dispersion relation $\omega_{\mathbf{q}}$ is plotted in blue. The dielectric constant of the substrate layers ($\epsilon_1 = \epsilon_2 = 1$), and the height $h = 8\text{\AA}$ are kept constant. The dielectric constant of the 2D layer ϵ_0 and $\omega_{\mathbf{q}}$ are given in the descriptions.

From the colorbars, it is clear that there is a decrease in EELS intensity for increasing internal screening, which means there is a dampening of the plasmonic excitation. Also, we notice that the energy per \mathbf{q} point decreases with increasing interband screening.

4.3 Varying height

In this section, we will look at the effect of the height of the 2D layer. This is achieved by comparing different internal screening cases at two different heights, $h = 4.0\text{\AA}$ and $h = 8.0\text{\AA}$. In Figure 9, the full EELS is shown for different 2D layer dielectric constants ϵ_0 and height h .

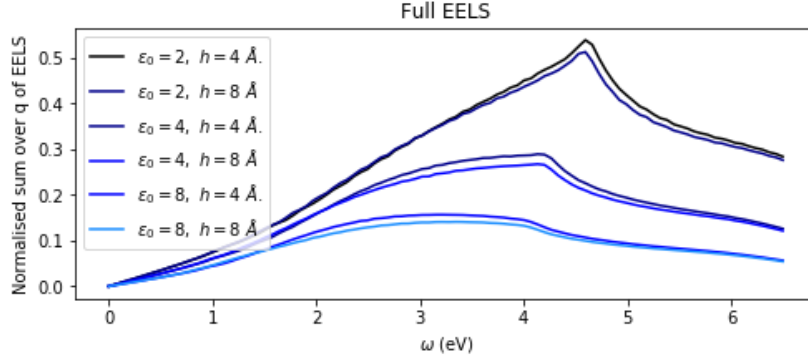


Figure 9: The full EELS for different internal screening cases, i.e. varying ϵ_0 , at different heights h . The dielectric constant of the substrate layers are kept constant, $\epsilon_1 = \epsilon_2 = 1$.

As explained in section 4.1, if $\epsilon_0 = \epsilon_1 = \epsilon_2$ the dielectric function is no longer dependent on the height of the 2D layer. This means that there is no difference in the EELS between varying heights for this case. For this reason, $\epsilon_0 = \epsilon_1 = \epsilon_2 = 1$ is not shown in Figure 9.

In the figure we see that increasing the 2D layer height results in a reduction of the full EELS intensity. This indicates a dampening of the plasmonic excitation. In Figure 10, colormaps of the EELS are shown for a height of $h = 4\text{\AA}$. These figures are overlain with the fitted plasmon dispersion $\omega_{\mathbf{q}}$ as found in the corresponding (same dielectric constants but different height $h = 8\text{\AA}$) figures in section 4.2, to visualize the change in EELS for smaller 2D layer height.

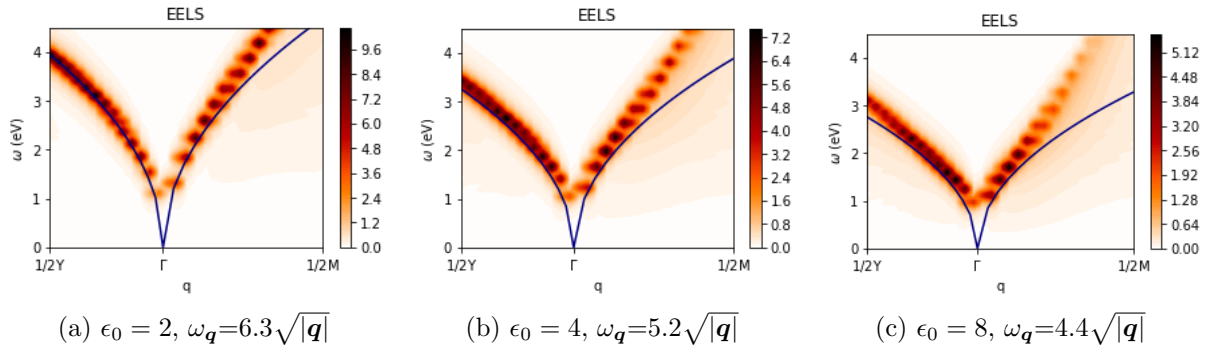


Figure 10: In each figure, the $EELS_{\mathbf{q}}(\omega)$ is shown as a colormap along paths towards high symmetry points in a square lattice. The 2D layer has a dielectric constant ϵ_0 and a height $h = 4\text{\AA}$. The dielectric constant of the substrate layers is kept constant, $\epsilon_1 = \epsilon_2 = 1$. In blue, a fitted simple plasmon dispersion $\omega_{\mathbf{q}}$ is plotted for the corresponding $h = 8\text{\AA}$ case.

Comparing the values of the EELS here, with the values in Figure 8, we again see an increase in EELS intensity for decreasing height, as we found in Figure 9. Also, by comparing the fitted dispersion with the maximal EELS, we see that for a thinner 2D layer, we have a slightly higher plasmon energy at a certain \mathbf{q} point, for small momenta. This can be explained by the behaviour of the effective dielectric function $\epsilon_{\mathbf{q}}$, see Figure 2. In this figure we saw that, with decreasing height, $\epsilon_{\mathbf{q}}$ grows less fast (i.e. has a flatter increase) for small \mathbf{q} vectors. This results in a slightly larger partially screened Coulomb interaction $U_{\mathbf{q}}$ and therefore, a larger plasmon energy.

4.4 External screening

In this section, the effect of the external screening channel on the plasmon dispersion will be examined. This is achieved by keeping the dielectric constant ϵ_0 and the height h of the 2D layer constant and varying the dielectric constant of the top and bottom substrate simultaneously. These variations are shown in Figure 11. Also, for each figure, a simple dispersion relation is fitted to visualize the differences. Note that the fitted plasmon dispersion $\omega_q = c\sqrt{q}$ is only correct for the perfect 2D electron gas. We are no longer considering a similar case, so the fitted dispersion are only there to make comparing the different pictures easier.

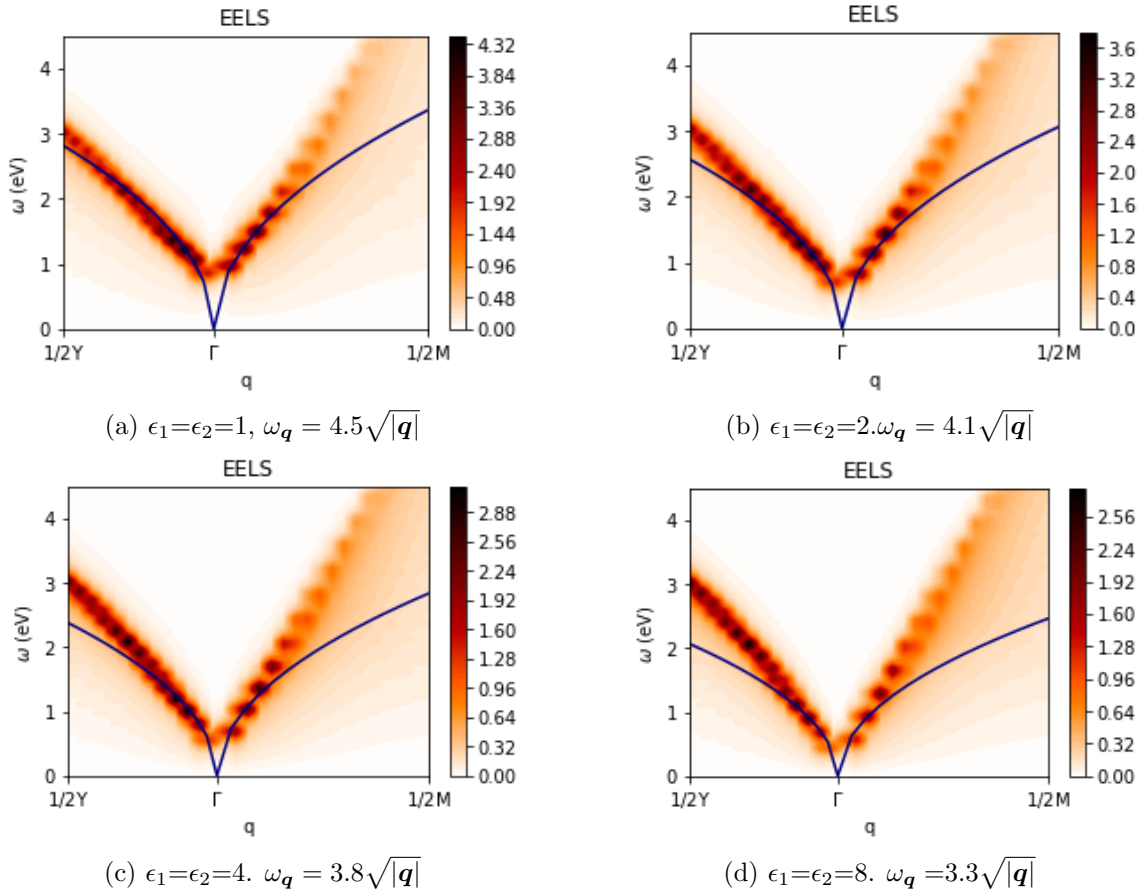


Figure 11: Each figure shows a colormap of $EELS_{\mathbf{q}}(\omega)$ along a path towards high symmetry point in the square lattice. The corresponding fitted dispersion relations $\omega_{\mathbf{q}}$ are plotted in blue. The dielectric constant of the 2D layer is kept constant: $\epsilon_0 = 8$. The dielectric constants of the substrate layers ϵ_1, ϵ_2 and the fitted dispersion $\omega_{\mathbf{q}}$ are given in the descriptions. The height of the 2D layer is 8\AA .

The first thing we again notice, is the decrease in EELS intensity for increasing ϵ_1, ϵ_2 . This means that for an increase in external screening, the plasmon dampens.

Next, we see a change in the shape of the fitted plasmon dispersions. The plasmon energy at a certain \mathbf{q} point decreases drastically with increasing screening for small \mathbf{q} . This can again be explained by the behaviour of the effective dielectric function $\epsilon_{\mathbf{q}}$, see Figure 2. Here we saw that with increasing screening (i.e. larger dielectric substrate constants ϵ_1, ϵ_2) the effective dielectric function $\epsilon_{\mathbf{q}}$ has a higher value for $\mathbf{q} = 0$. If the effective dielectric function is larger, the screened Coulomb interaction decreases, and with it, the plasmon energy.

4.5 Anisotropy

In this section, the effect of an anisotropic screening channel on the plasmon is investigated. For this, the dielectric constant and height of the 2D layer material are kept constant and anisotropy is only added through the external screening channels by simultaneously varying the dielectric constants of the substrate layers. In Figure 12, the results are visualised. Here, the EELS is shown as a colormap over the path $\frac{1}{2}X - \Gamma - \frac{1}{2}Y$. If the external screening is isotropic, as in Figure 12a, the EELS is symmetric. For this case, a dispersion relation is fitted. The same dispersion is shown in the anisotropic plots (Figures 12b till 12d).

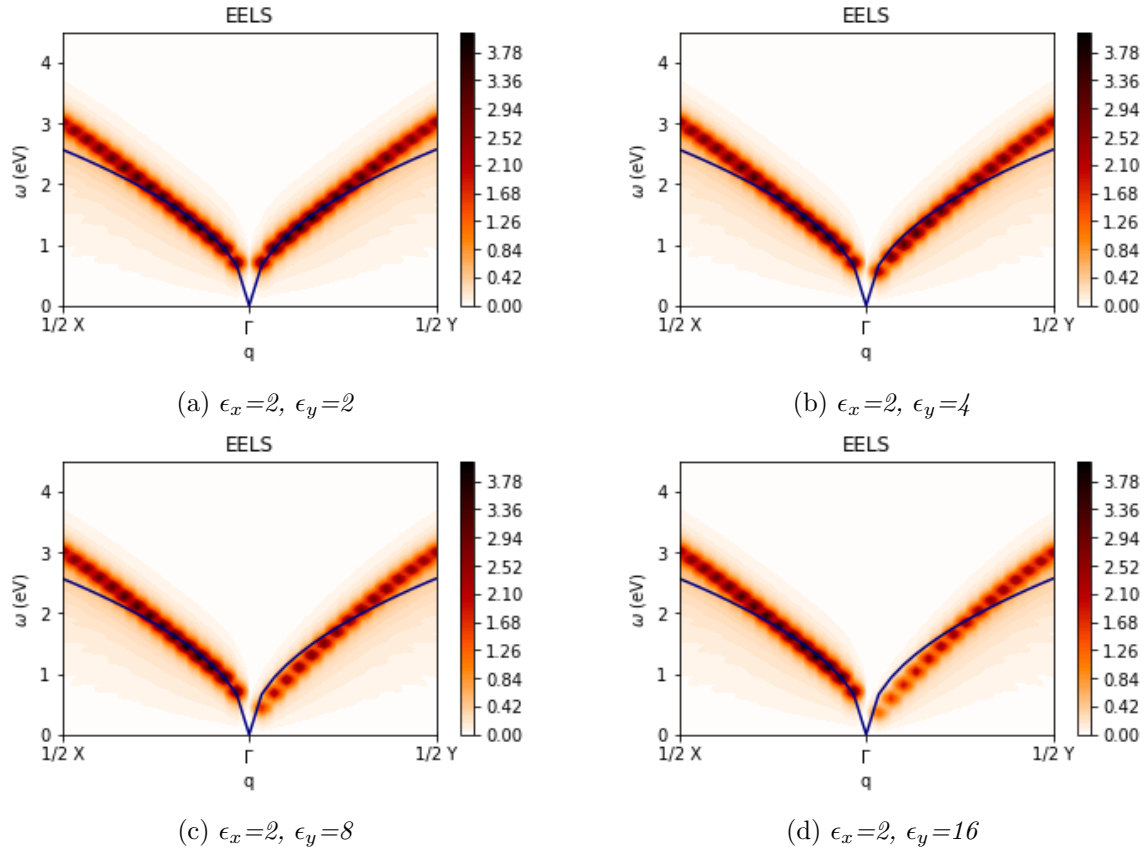


Figure 12: $EELS_{\mathbf{q}}(\omega)$ as a colormap along paths towards high symmetry points in a square lattice. The colormaps are made for increasing anisotropy, caused by external screening (varying ϵ_1, ϵ_2). Both ϵ_1 and ϵ_2 have the same constant x-component ($\epsilon_x=2$.) and varying y-component ϵ_y . The dielectric constant of the material layer is kept constant at $\epsilon_0=8$. In blue, the dispersion relation $\omega_{\mathbf{q}} = 4.1\sqrt{|\mathbf{q}|}$ is fitted. This dispersion corresponds to the maximum of the EELS in the isotropic picture in figure (a). The height of the material layer is 8\AA .

In Figure 12, the screening in the Y direction is increased in the successive pictures³. This creates a directional dependence, i.e. anisotropy, of the EELS and therefore, of the plasmon dispersion. The increase in Y-screening dampens the plasmon, which can be seen by the lowering in intensity of the EELS in the Y direction. Note that this change is only in the Y direction, the X direction is unchanged. This shows us that anisotropic plasmon excitations can be induced in a isotropic 2D metallic layer in a non-invasive way; we only add anisotropic substrate screening, the 2D layer itself remains unchanged.

Also, we see a decrease in energy for a given wave vector in the Y direction in Figure 12.

³Note that the dispersion in Figure 12a is the same as in Figure 11b. These figures show the exact same situation, just over different paths.

This results in a decrease in the energy needed to excite an electron at a certain wave vector. Note how the EELS above the dispersion does not change shape, only intensity. This can be explained by the fact that the plasmon there is already very close to, or already on top of the polarization. Therefore, the plasmon is no longer well defined there.

5 Conclusion and outlook

For this report, an implementation was made for the plasmon calculations in a one orbital tight binding model of a 2D square lattice. This was made mostly from scratch using the freely available TPRF framework [11]. An important part of this implementation was the WFCE Coulomb interaction, which allowed us to use only the metallic polarization term, by realistically compensating for the other screening channels.

With this implementation, the effect of material parameters on the plasmonic excitations were studied. When increasing the screening in any one of the screening channels, the intensity of the EELS decreases, and with it, the plasmonic excitations are dampend. Also, increasing the 2D layer height will dampen the plasmonic excitation. This effect seems to be much smaller than changing the screening. To quantify this, more calculations have to be done.

Finally, the implementation was used to investigate whether we can induce anisotropic plasmonic excitations in a isotropic 2D metal. To do this, the substrate layers above and below the 2D metal were made anisotropic. It was found that the screening resulting from the anisotropic substrate layers indeed resulted in an anisotropic plasmonic excitation in the 2D metal.

To improve on these results, more computational power is needed. The results will get more precise for a denser \mathbf{q} -grid, but increasing the \mathbf{q} -grid increases computing time exponentially. An other way to enhance the results is to improve on the precision of the metal polarization. This can be done by strongly decreasing the temperature (increase β) and decreasing the broadening parameter δ . This has to be done in combination with a denser \mathbf{q} -grid, because a smaller δ in the same \mathbf{q} -grid will result in more variations of the results, making it harder to interpret.

Lastly, we would like to note that, a start was made to Fourier transform these results to real space. This code can also be found in the git repository [13].

A Code

The code is structured into 3 files; `squareComputation.py`, `compDefinition.py`, and `plotfile.py`. The first file contains the "main" implementation. Here all important physical quantities, like the Hamiltonian, polarization, dispersions and Coulomb interactions, are defined. The file imports the `compDefinition.py` file, which contains the self written functions needed for calculating the physical quantities. The file `plotfile.py` is used to create all plots found in this report. It also holds the definitions of the symmetry points and some functions used to create (quantities over) paths between these points. Quantities from `squareComputation.py` are conveyed to `plotfile.py` using `HDFArchive`.

In this appendix, some functions from `compDefinition.py` are shown with additional comments.

Below the implementation of the bare Coulomb interaction (equation (1)) is given. Note that a different front factor is used as in equation (1). This is to ensure the Coulomb interaction is the same units as the rest of the program. The program is defined in units of eV and Å. Also, a case needed to be added to the function to solve the problem of division by 0.

```
def bare_coulomb(qvec,A):
    """ Calculation of bare coulomb interaction:  $V_q = c/|q|$ 
    The case is added to allow a  $|q|$  of 0 """
    q = np.linalg.norm(qvec.value)
    if q == 0.0:
        V_q = 2*np.pi*14.399/A *1/0.0000000001
    else:
        V_q = 2*np.pi*14.399/A * 1/q
    return V_q
```

The next function calculates the effective dielectric function and is the implementation of equations (10), (11) and (12).

```
def get_eq(e1,e2,e3,h,q):
    """ Calculation of dielectric constant  $e_q$ .
    Can take in a constant or a vector for  $e2/3$  """
    q_norm = np.linalg.norm(q.value)

    if q_norm == 0.:
        return e1
    else:
        if not isinstance(e2,float) :
            # e2 is anisotropic
            e2 = [[e2[0],0.],[0.,e2[1]]]
            dot = np.dot(e2,[q.value[0],q.value[1]])
            e2 = np.linalg.norm(dot)/q_norm
        if not isinstance(e3,float):
            # e3 is anisotropic
            e3 = [[e3[0],0.],[0.,e3[1]]]
            dot = np.dot(e3,[q.value[0],q.value[1]])
            e3 = np.linalg.norm(dot)/q_norm

    e2t = (e1-e2) / (e1+e2) #e2 tilde
    e3t = (e1-e3) / (e1+e3) #e3 tilde
    num = e1*( 1. - e2t*e3t*np.exp(-2.*q_norm*h) )
    denom = 1. + (e2t+e3t)*np.exp(-q_norm*h)
```

```

denom += e2t*e3t*np.exp(-2.*q_norm*h)
eq = num / denom
return eq

```

For completeness, also the implementation of the screened Coulomb interaction, equation (9), is given.

```

def WFCE_coulomb(kmesh,gsize,e1,e2,e3,h,A):
    """ Calculation of substrate adjusted coulomb interaction:
        U_q = V_q/e_q """
    V_q = np.empty(gsize*gsize)
    e_q = np.empty(gsize*gsize, dtype=np.complex)
    for qvec in kmesh:
        e_q[qvec.linear_index] = get_eq(e1,e2,e3,h,qvec)
        V_q[qvec.linear_index] = bare_coulomb(qvec,A)
    U_q = V_q / e_q
    return U_q,V_q

```

References

- [1] H. Bruus; K. Flensberg. *Many-body quantum theory in condensed matter physics - an introduction*. Online book. 2002.
- [2] A. Bill; H. Morawitz; V.Z. Kresin. ‘Electronic collective modes and superconductivity in layered conductors’. In: *Phys. Rev. B* (2003). DOI: 10.1103/PhysRevB.68.144519.
- [3] W. Barnes; A. Dereux; T. Ebbesen. ‘Surface plasmon subwavelength optics’. In: *Nature* (2003). DOI: 10.1038/nature01937.
- [4] A.N. Grigorenko; M. Polini; K.S. Novoselov. ‘Graphene plasmonics’. In: *Nature Photonics* (2012). DOI: 10.1038/nphoton.2012.262.
- [5] M. Rösner. ‘Electronic Structure of Novel Two-dimensional Materials and Graphene Heterostructures’. Doctoral dissertation. Universität Bremen, 2016.
- [6] G. Schönhoff; M. Rösner; R.E. Groenewald; S. Haas; T.O. Wehling. ‘Interplay of screening and superconductivity in low-dimensional materials’. In: *Physical review B* (2016). DOI: 10.1103/PhysRevB.94.134504.
- [7] R.E. Groenewald; M. Rösner; G. Schönhoff; S. Haas; T.O. Wehling. ‘Valley plasmonics in transition metal dichalcogenides’. In: *Physical review B* (2016). DOI: 10.1103/PhysRevB.93.205145.
- [8] R. F. Egerton. ‘Electron energy-loss spectroscopy in the TEM’. In: *Reports on Progress in Physics* (2008). DOI: 10.1088/0034-4885/72/1/016502.
- [9] T. Westerhout; E. van Veen; M.I. Katsnelson; S. Yuan. ‘Plasmon confinement in fractal quantum systems’. In: *Phys. Rev. B* (2018). DOI: 10.1103/PhysRevB.97.205434.
- [10] H.U.R. Strand. *Square lattice susceptibility and the Random Phase Approximation (RPA) - TPRF*. https://triqs.github.io/tprf/latest/user_guide/Square%20lattice%20susceptibility.html?highlight=hamiltonian.
- [11] H.U.R. Strand. *TPRF (two-particle response function tools)*. v2.2. <https://triqs.github.io/tprf/latest/>.
- [12] P. Hofmann. *Solid State Physics - An Introduction*. Second edition. Wiley-VCH, 2015.
- [13] A.H.A. Riewald. *2020_Riewald_2D_plasmons*. <https://gitlab.science.ru.nl/roesner/bachelor>.
- [14] W. H. Backes et al. ‘Dispersion of longitudinal plasmons for a quasi-two-dimensional electron gas’. In: *Phys. Rev. B* (1992). DOI: 10.1103/PhysRevB.45.8437.